Advanced Studies in Theoretical Physics
Vol. 15, 2021, no. 5, 257 - 266
HIKARI Ltd, www.m-hikari.com
https://doi.org/10.12988/astp.2021.91652

The Effect of the Leak Conductance Parameter on the Dynamics of a Mathematical Model of pre-Bötzinger Complex Pacemaker Neurons: Period-Doubling Bifurcation and Chaotic Activity

Takaaki Shirahata

Kagawa School of Pharmaceutical Sciences
Tokushima Bunri University
1314-1 Shido, Sanuki, Kagawa 769-2193, Japan

Abstract

The present article presents results of a numerical simulation of a mathematical model of pre-Bötzinger complex pacemaker neurons, which is described by a system of nonlinear ordinary differential equations. A controlling parameter of the present study was leak conductance contained in the pre-Bötzinger complex pacemaker neuron model. In addition, we numerically investigated the effect of variation of that parameter on the dynamics of the model. Numerical simulation results indicated that an increase in leak conductance changes the dynamical state of the model, such that a period-1 spiking state → a period-2 spiking state → a period-4 spiking state → a chaotic spiking state → a chaotic bursting state → a periodic bursting state.

Mathematics Subject Classification: 37N25, 92C20

PACS: 05.45.-a, 87.19.ll

Keywords: mathematical model, pre-Bötzinger complex pacemaker neurons, leak conductance, period-doubling bifurcation, chaotic

1 Introduction

Pre-Bötzinger complex pacemaker neurons are capable of exhibiting bursting activity, and a previous study has proposed a mathematical model to reproduce this activity [1]. The model is an example of a nonlinear system and is described by a system of nonlinear ordinary differential equations (ODEs) based on the Hodgkin–Huxley formalism. This pre-Bötzinger complex pacemaker neuron model is highly sensitive to parameter variations. For example, the transient current pulse injection can reset the model's bursting cycle [1, 2]. Furthermore, parameters describing leakage current are important for changing the dynamical state of the model: variations in leakage reversal potential or leak conductance can induce dynamical state changes, such that a hyperpolarized steady state leads to a bursting state, resulting in a spiking state [1, 3]. According to the textbook of computational neuroscience, understanding the bifurcation that leads to bursting dynamics is important [4]. Therefore, it is necessary to understand the type of bifurcation involved in the transition between the bursting and spiking state in the pre-Bötzinger complex pacemaker neuron model. A previous study of this model investigated bifurcation in detail, whereby the change in the parameter describing a long-lasting current pulse injection (which is essentially identical to the change in the leakage reversal potential) induced the transition between a bursting and spiking state [5]. However, bifurcation, whereby the change in leak conductance induces transition, has not yet been studied in detail. Therefore, it is important to elucidate bifurcation that is induced by leak conductance. The pre-Bötzinger complex pacemaker neuron model is classified into models 1 and 2 [1]. A previous study suggested that model 1 is more experimentally realistic [1]. Thus, we numerically investigated the effect of variation in leak conductance on the dynamics of model 1.

2 Mathematical model of pre-Bötzinger complex pacemaker neurons

The present study investigated model 1 of pre-Bötzinger complex pacemaker neurons that is described by the following system of three coupled nonlinear ODEs:

$$\frac{dV}{dt} = \frac{1}{C}\left[-I_{NaP}(V,h) - I_{Na}(V,n) - I_K(V,n) - I_L(V)\right] \tag{1}$$

$$\frac{dn}{dt} = \frac{1}{\tau_n(V)}\left[n_\infty(V) - n\right] \tag{2}$$

$$\frac{dh}{dt} = \frac{1}{\tau_h(V)}\left[h_\infty(V) - h\right] \tag{3},$$

where V (mV; the membrane potential of the neurons), n (the gating variable of

the activation of the delayed-rectifier potassium conductance), and h (the gating variable of the inactivation of the persistent sodium conductance) are state variables; t (ms) is time; C (=21 pF) is the membrane capacitance; $I_{NaP}(V,h)$, $I_{Na}(V,n)$, $I_K(V,n)$, and $I_L(V)$ are the persistent sodium, fast sodium, delayed-rectifier potassium, and leakage currents, respectively (defined below); $\tau_n(V)$ and $\tau_h(V)$ are the time constants of n and h, respectively (defined below; $n_\infty(V)$ and $h_\infty(V)$ are the steady state (in)activation functions of n and h, respectively (defined below).

$$I_{NaP}(V,h) = 2.8\left(\frac{1}{1+e^{\frac{V+40}{-6}}}\right)h\left(V-50\right) \tag{4}$$

$$I_{Na}(V,n) = 28\left(\frac{1}{1+e^{\frac{V+34}{-5}}}\right)^3\left(1-n\right)\left(V-50\right) \tag{5}$$

$$I_K(V,n) = 11.2n^4\left(V+85\right) \tag{6}$$

$$I_L(V) = g_L\left(V-E_L\right) \tag{7}$$

$$\tau_n(V) = \frac{10}{\cosh\frac{V+29}{-8}} \tag{8}$$

$$n_\infty(V) = \frac{1}{1+e^{\frac{V+29}{-4}}} \tag{9}$$

$$\tau_h(V) = \frac{10000}{\cosh\frac{V+48}{12}} \tag{10}$$

$$h_\infty(V) = \frac{1}{1+e^{\frac{V+48}{6}}} \tag{11},$$

where g_L (nS; the leak conductance) and E_L (mV; the leakage reversal potential) are the controlling parameters. In the present study, E_L was fixed at –65 mV, and g_L was changed. Equations (1)–(11) were numerically solved using the free open-source software Scilab (http://www.scilab.org/) under the following initial condition: V = –51 mV, n = 0.005, and h = 0.4722. Details of the equations are explained in a previous publication [1].

3 Numerical Results

The present study focused on the controlling parameter, g_L, and we numerically studied the effect of increased g_L on the dynamics of model 1 of pre-Bötzinger complex pacemaker neurons. The time course of V and the phase plane trajectory indicated that when g_L was 1.12 nS, model 1 demonstrated a period-1 spiking state;

the membrane potential oscillation of period-1 was observed (Figure 1). When g_L was increased to 1.14 nS, model 1 demonstrated a period-2 spiking state; the membrane potential oscillation of period-2 was observed (Figure 2). When g_L was further increased to 1.141 nS, model 1 demonstrated a period-4 spiking state; the membrane potential oscillation of period-4 was observed (Figure 3). In all cases, model 1 exhibited periodic activity. Contrarily, when g_L was further increased to 1.1469 nS, model 1 showed a chaotic spiking state; the period of membrane potential oscillation was irregular (Figure 4). When g_L was further increased to 1.1474 nS, model 1 similarly showed a chaotic state (i.e., a chaotic bursting state) (Figure 5); however, the type of chaotic activity differed from that observed in Figure 4. The bursting state consisted of two phases: spiking and resting. In a chaotic bursting state, as presented in Figure 5, we observed that the duration of the spiking phase was irregular (Figure 5a). As the bursting state consisted of two phases, the phase plane trajectory was complex (Figure 5b). To evaluate the trajectory in detail, the range of the horizontal axis (i.e., h) of the phase plane was expanded (Figure from 5c to 5f). Specifically, when we focused on a small h (i.e., h ranged from approximately 0.343–0.346), we observed a chaotic trajectory (Figure 5f). When g_L was further increased to 1.18 nS, model 1 demonstrated a periodic bursting state (Figure 6). Contrary to Figure 5, we observed that the duration of the spiking phase was regular (Figure 6a). The phase plane trajectory of the periodic bursting state (Figure 6b) was visually similar to that of the chaotic bursting state observed in Figure 5b. However, as was observed in Figure 5c–f, when the range of the horizontal axis (i.e., h) of the phase plane was expanded (Figure 6c–f), the difference in the trajectory between the chaotic and periodic bursting states became clear; although a large portion of the trajectory was similar between the chaotic and periodic bursting states when we focused on a large h (i.e., h larger than approximately 0.36 in Figures 5c, 5d, 5e, 6c, 6d, and 6e), a specific small section of the trajectory significantly differed between the two states when we focused on a small h (i.e., h ranging from approximately 0.343–0.346 and from 0.353 to 0.355 in Figures 5f and 6f, respectively).

4 Conclusion

From the point of view of a nonlinear dynamical system, it is important to understand bifurcation, whereby a system changes between a spiking and bursting state, to elucidate whether a chaotic state occurs during the transition process between these two states [4]. A previous study of model 1 of pre-Bötzinger complex pacemaker neurons indicated that the transition from a bursting to a spiking state induced by variations in the long-lasting current pulse injection occurred by the coalescence of two saddles and the remainder of only one fixed point (stable focus) in the system [5]. However, the previous study did not reveal whether a chaotic state was involved in the transition. Our study indicated that chaotic states are involved in the transition between the spiking and bursting state. We showed that an increase in g_L changed the dynamical state of model 1, such that a period-1 spiking state → a period-2 spiking state → a period-4 spiking state

(i.e., period-doubling bifurcation) → a chaotic spiking state → a chaotic bursting state → a periodic bursting state. Previous studies of other mathematical models also clarified that chaotic states, such as chaotic spiking and chaotic bursting states, occur during the transition process between a spiking and bursting state [6-8]. However, the number of dimensions of the system in a previous study (i.e., eight dimensions [6]) was different from that of the present study (three dimensions), whereas those studied in [7, 8] had the same number dimensions (i.e., three dimensions) as the present study. Moreover, the type of slow variable of the system differed between previous studies [7, 8] and our study. Previous studies used activation of slow potassium conductance [7] or intracellular calcium concentration [8] as slow variables, whereas in our study, we used inactivation of persistent sodium conductance.

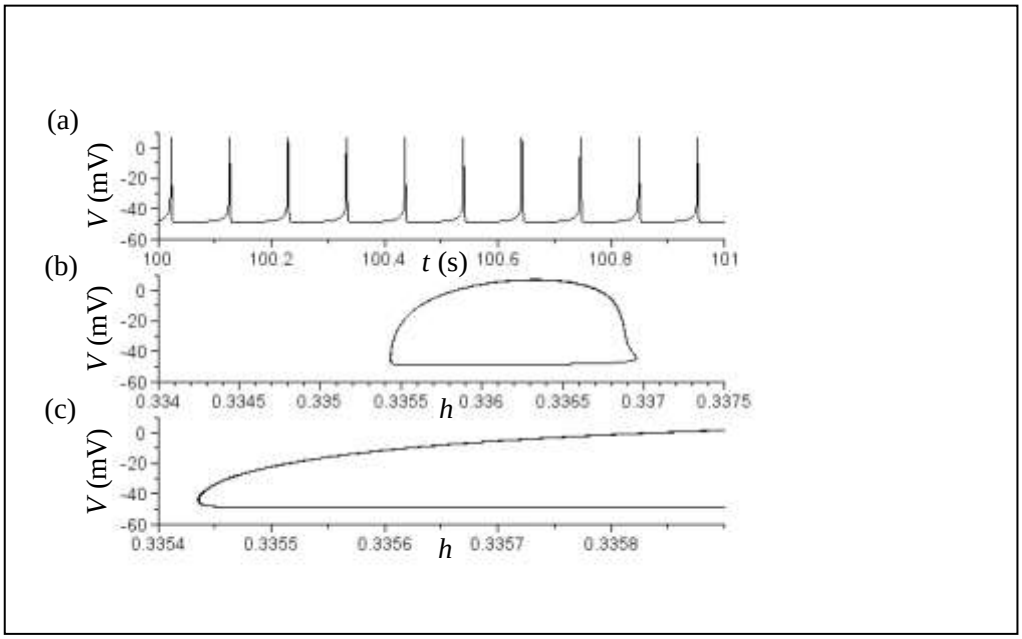

Figure 1. Period-1 spiking state of model 1. (a) Time course of V at g_L = 1.12 nS. (b) Phase plane trajectory (h, V) at g_L = 1.12 nS. (c) Expanded view of (b). Part of the trajectory within the range in which h is between 0.3354 and 0.3360.

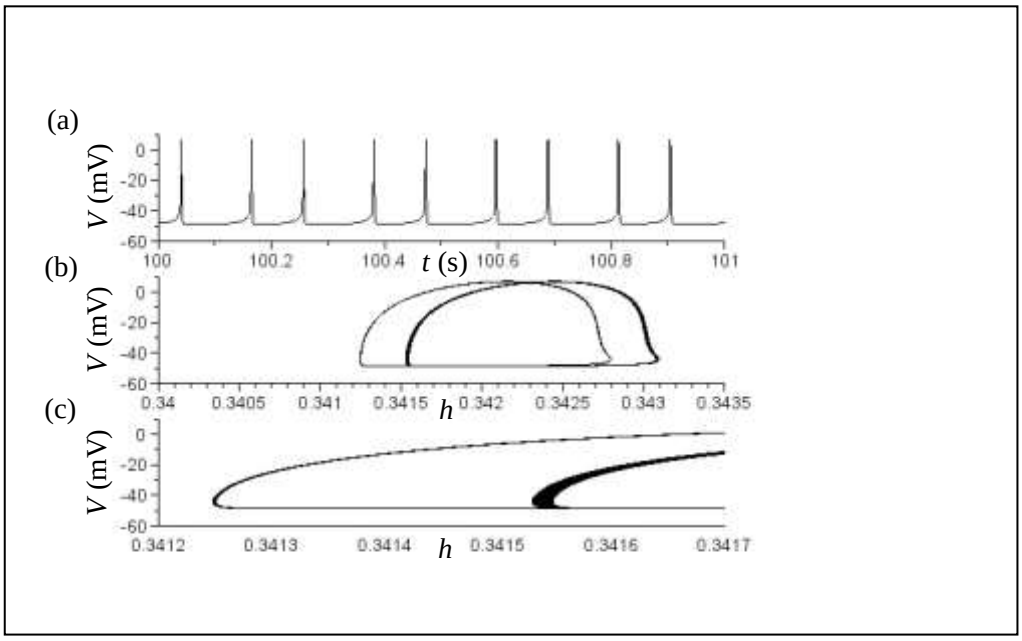

Figure 2. Period-2 spiking state of model 1. (a) Time course of V at g_L = 1.14 nS. (b) Phase plane trajectory (h, V) at g_L = 1.14 nS. (c) Expanded view of (b). Part of the trajectory within the range in which h is between 0.3412 and 0.3417.

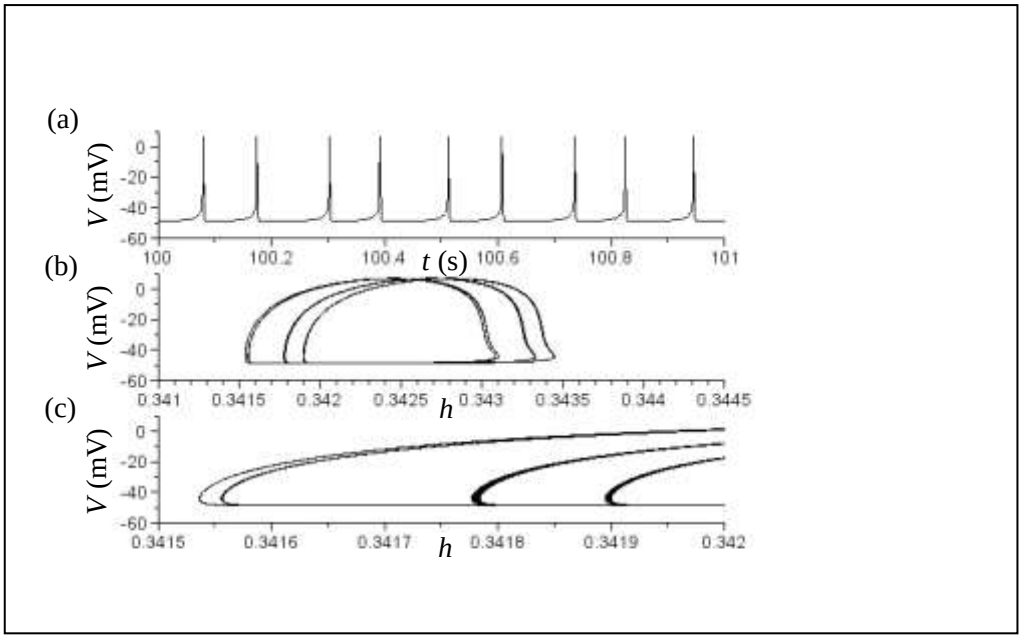

Figure 3. Period-4 spiking state of model 1. (a) Time course of V at g_L = 1.141 nS. (b) Phase plane trajectory (h, V) at g_L = 1.141 nS. (c) Expanded view of (b). Part of the trajectory within the range in which h is between 0.3415 and 0.3420.

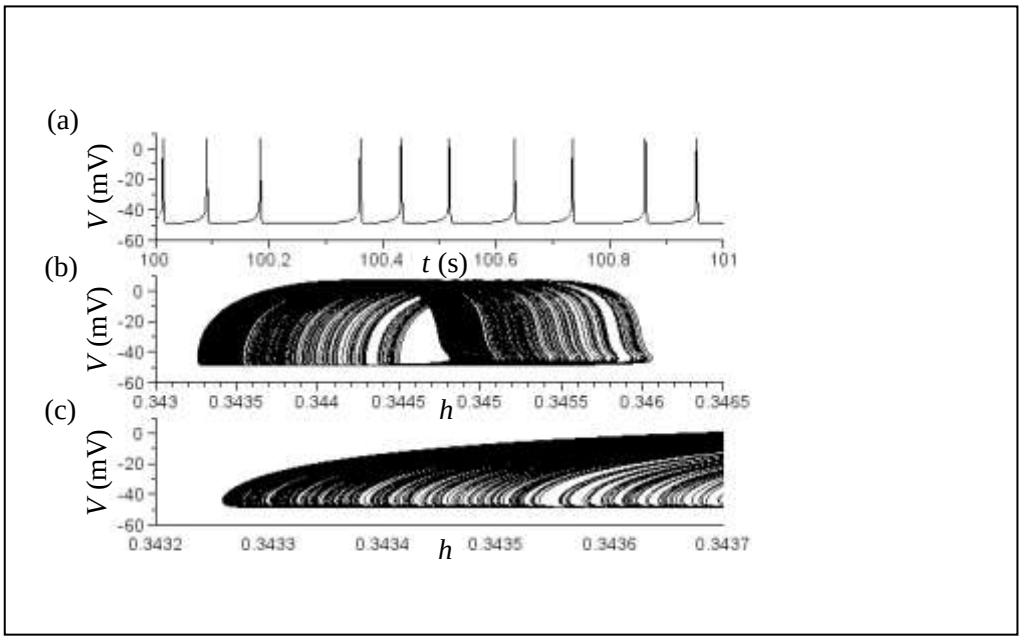

Figure 4. Chaotic spiking state of model 1. (a) Time course of V at g_L = 1.1469 nS. (b) Phase plane trajectory (h, V) at g_L = 1.1469 nS. (c) Expanded view of (b). Part of the trajectory within the range in which h is between 0.3432 and 0.3437.

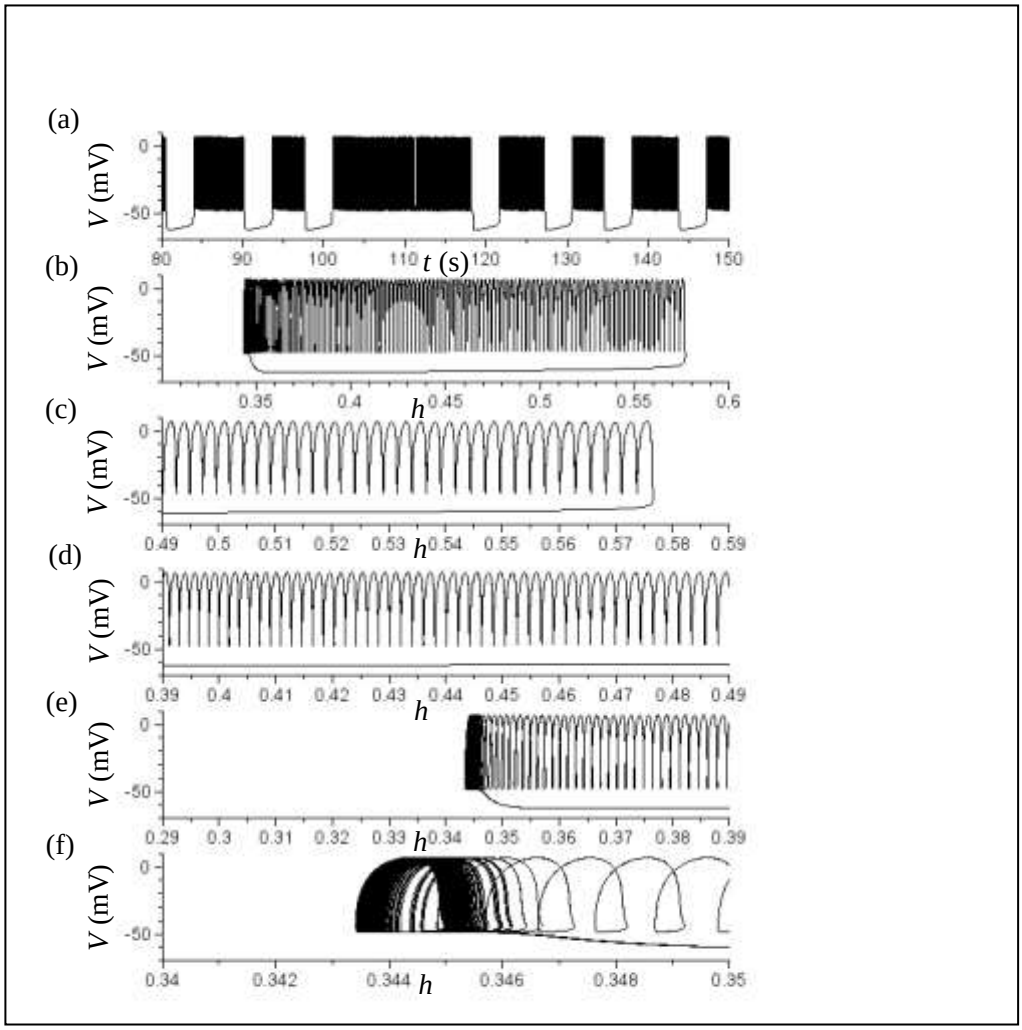

Figure 5. Chaotic bursting state of model 1. (a) Time course of V at g_L = 1.1474 nS. (b) Phase plane trajectory (h, V) at g_L = 1.1474 nS. (c–e) Expanded view of (b). Part of the trajectory within the range in which h is between 0.49 and 0.59 (c), between 0.39 and 0.49 (d), and between 0.29 and 0.39 (e). (f) Expanded view of (e). Part of the trajectory within the range in which h is between 0.34 and 0.35.

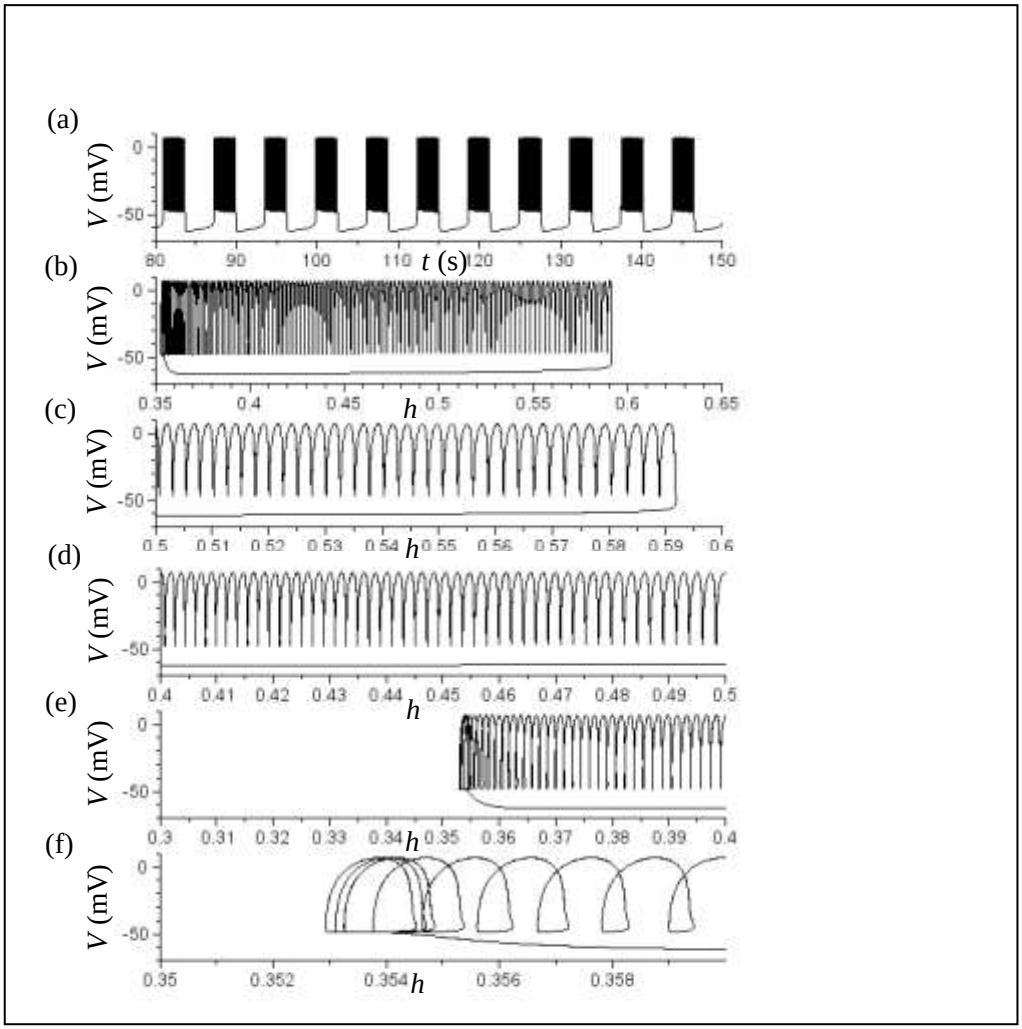

Figure 6. Periodic bursting state of model 1. (a) Time course of V at g_L = 1.18 nS. (b) Phase plane trajectory (h, V) at g_L = 1.18 nS. (c–e) Expanded view of (b). Part of the trajectory within the range in which h is between 0.50 and 0.60 (c), between 0.40 and 0.50 (d), and between 0.30 and 0.40 (e). (f) Expanded view of (e). Part of the trajectory within the range in which h is between 0.35 and 0.36.

Acknowledgements. The author would like to thank Enago (www.enago.jp) for the English language review.

References

[1] Butera, R. J., Rinzel, J., and Smith, J.C., Models of respiratory rhythm generation in the pre-Botzinger complex. I. Bursting pacemaker neurons, *Journal of Neurophysiology*, **82** (1999), 382-397. https://doi.org/10.1152/jn.1999.82.1.382

[2] Shirahata, T., The effect of hyperpolarizing inputs on the dynamics of a bursting pacemaker neuron model in the pre-Bötzinger complex, *Neuroscience Letters*, **473** (2010), 16-21. https://doi.org/10.1016/j.neulet.2010.02.010

[3] Del Negro, C. A., Koshiya, N., Butera, R. J., and Smith, J. C., Persistent sodium current, membrane properties, and bursting behavior of pre-Botzinger complex inspiratory neurons in vitro, *Journal of Neurophysiology*, **88** (2002), 2242-2250. https://doi.org/10.1152/jn.00081.2002

[4] Izhikevich, E. M., *Dynamical Systems in Neuroscience*, The MIT Press, Cambridge, Massachusetts, 2007. https://doi.org/10.7551/mitpress/2526.001.0001

[5] Cordovez J. M., Wilson C. G., and Solomon I. C., Geometrical analysis of bursting pacemaker neurons generated by computational models: comparison to in vitro pre-Bötzinger complex bursting neurons, *Advances in Experimental Medicine and Biology*, **669** (2010), 45-48. https://doi.org/10.1007/978-1-4419-5692-7_9

[6] Shirahata, T., The transition from a periodic spiking state to a periodic bursting state via a chaotic bursting state: a numerical study of a dynamical system in neurobiophysics, *Advanced Studies in Theoretical Physics*, **14** (2020), 151-160. https://doi.org/10.12988/astp.2020.91462

[7] Medvedev, G. S., Transition to Bursting via Deterministic Chaos, *Physical Review Letters*, **97** (2006), 048102. https://doi.org/10.1103/physrevlett.97.048102

[8] Ermentrout, G. B. and Terman, D., *Mathematical Foundations of Neuroscience*, Springer, New York, 2010. https://doi.org/10.1007/978-0-387-87708-2

Received: May 12, 2021; Published: June 11, 2021